

See discussions, stats, and author profiles for this publication at: <https://www.researchgate.net/publication/260106702>

Theoretical study of the electronic structure of LiX and NaX (X = Rb, Cs) molecules

ARTICLE *in* INTERNATIONAL JOURNAL OF QUANTUM CHEMISTRY · AUGUST 2012

Impact Factor: 1.43 · DOI: 10.1002/qua.23295

CITATIONS

7

READS

26

4 AUTHORS, INCLUDING:



Riadh Dardouri

University of Monastir

8 PUBLICATIONS 24 CITATIONS

SEE PROFILE



Brahim Oujia

University of Monastir

61 PUBLICATIONS 296 CITATIONS

SEE PROFILE



Florent Xavier Gadéa

Paul Sabatier University - Toulouse III

153 PUBLICATIONS 2,818 CITATIONS

SEE PROFILE

Theoretical Study of the Electronic Structure of LiX and NaX (X = Rb, Cs) Molecules

Riadh Dardouri,^{*,[a]} Khaled Issa,^[a] Brahim Oujia,^[a] and Florent Xavier Gadéa^[b]

Adiabatic potential energy, spectroscopic constants, dipole moments, and vibrational levels have been computed for the lowest electronic states of alkali dimers LiX and NaX (X = Rb, Cs). Calculations have been carried with the use of an *ab initio* approach with core-potential potentials and full-valence configuration. Thus, these systems are treated as two-electron systems. A good agreement is obtained for

some lowest states of the molecules studied with available theoretical works. The existence of numerous avoided crossings between electronic states for $^1\Sigma$ symmetries is related to the charge-transfer process in each molecule between its two ionic systems (Li^+X^- , Li^-X^+) and (Na^+X^- , Na^-X^+). © 2011 Wiley Periodicals, Inc. *Int J Quantum Chem* 000:000–000, 2011

Keywords: adiabatic approximation · pseudo-potential · core valence correlations · full valence CI approach · spectroscopic constants · crossings · vibrational levels

Introduction

A considerable interest has been focused on the photo-associative spectroscopy of cold alkali atoms,^[1] and more recently, on cold molecule formation^[2] due to spectacular applications such as manipulation and controlling of ultra-cold chemical reactions,^[3–5] ultra-cold molecular collision dynamics,^[6–9] quantum computing,^[10,11] and preparation of few-body quantum effects.^[12] The aim of this research field is to prepare molecules in definite quantum states with respect to the center of mass, electronic, rotational, and vibrational motions. Indeed, ultra-cold molecules^[13,14] offer many new opportunities compared with ultra-cold atoms. The reason is that complex structures can carry an amount of internal energy larger by orders of magnitude than their kinetic energy. This opens new ways in ultra-cold photochemistry.^[15]

Theoretically, several methods have been used to study alkali dimers. Most of them proposed to reduce the number of electrons only to valence electrons by using pseudopotentials. The use of pseudopotentials for Li, Na, Rb, and Cs cores reduces the number of active electrons to only one valence electron, where a self-consistent field calculation produces the exact energy in the basis and the main source of errors corresponds to the basis-set limitations. Furthermore, we correct the energy by taking into account the core–core and core–electron correlations following the formalism of Foucrault et al.^[16] This formalism was used first for Rb₂ and RbCs molecules and later for several systems (KH, RbH, CsH, NaH, LiNa, LiNa⁺, LiRb, and NaRb) and its use has proved to be efficient. The nonempirical pseudopotentials permit the use of very large basis sets for the valence and Rydberg states and allow accurate descriptions of the highest excited states.

The neutral molecules LiX and NaX have been investigated in many theoretical^[17–22] and experimental^[23–28] studies. The molecules are assumed to be a simplest heteromolecular with a one active electron. For all of them, we have obtained a re-

markable accuracy, showing the validity of this approach. The results obtained for LiX and NaX systems can be expected to reach a similar accuracy because the main restriction in the accuracy of calculations is the limitation in the basis set.

This article is organized as follows: after a brief introduction, we present, in “Details of Computations” section, the computational method. Results are discussed in “Results” section. Concluding remarks are summarized in the latter “Conclusions” section.

Details of Computations

In this study, the Li, Na, and X atoms are treated through the one-electron pseudopotential proposed by Barthelat et al.^[29,30] and used in many previous works (see, e.g., Refs. [31–34]). In addition, we take into account the core-valence correlation in view of the operator formalism of Muller et al.,^[35] written as

$$V_{\text{CPP}} = -\frac{1}{2} \sum_{\lambda} \alpha_{\lambda} \vec{f}_{\lambda} \vec{f}_{\lambda} \quad (1)$$

The summation runs over all the polarizable cores with a dipole polarizability. The electric field f is created on a center produced by valence electrons and all other cores, modified

[a] R. Dardouri, K. Issa, B. Oujia
Laboratoire de Physique Quantique, Université of Monastir, Faculté des Sciences de Monastir, Route de Kairouan 5019, Monastir, Tunisia
E-mail: dardourriad@yahoo.fr

[b] F. Xavier Gadéa
Laboratoire de Chimie et Physique Quantique, UMR5626 du CNRS, Université de Toulouse, UPS, 118 route de Narbonne, 31062 Toulouse Cedex 4, France


 Additional Supporting Information may be found in the online version of this article.

Table 1. *l*-Dependent cutoff radii (in Bohr) for the Li, Na, Rb, and Cs atoms.

L	Li	Na	Rb	Cs
s	1.433	1.44223	2.5134	2.7923
p	0.979	1.625	2.2985	2.667
d	0.600	1.5	2.5033	2.89575
f	0.400	1.5	2.51	2.81

by a cutoff function F with an l -dependent adjustable parameter

$$\vec{f}_\lambda = \sum_i \frac{\vec{r}_{i\lambda}}{r_{i\lambda}^3} F(r_{i\lambda}, \rho_\lambda) - \sum_{\lambda\lambda'} \frac{\vec{R}_{\lambda\lambda'}}{R_{\lambda\lambda'}^3} Z_{\lambda\lambda'} \quad (2)$$

where $r_{i\lambda}$ is a core-electron vector and $R_{\lambda\lambda'}$ is a core-core vector. The cutoff operator $F(r_{i\lambda}, \rho_\lambda)$ is expressed, following the Foucault formalism,^[16] by a step function defined by

$$F(r_{i\lambda}, \rho_\lambda) = (0, r_{i\lambda} < \rho_\lambda; 1, r_{i\lambda} > \rho_\lambda) \quad (3)$$

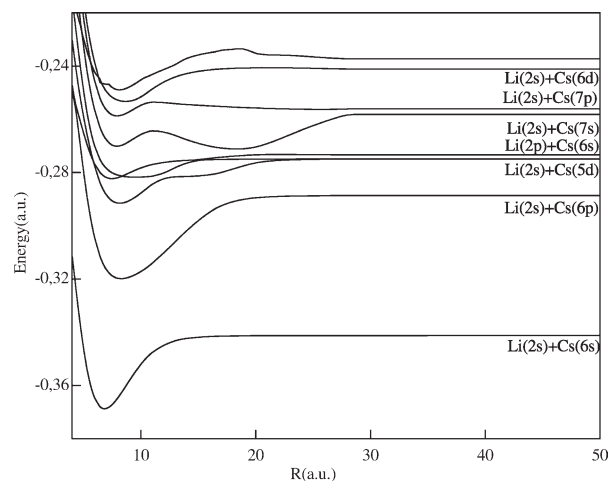
This has the physical meaning of excluding the valence electrons from the core region for calculating the electric field. The cutoff radius is taken to be a function of l as follows:

$$F(r_{i\lambda}, \rho_\lambda) = \sum_{l=0}^{\infty} \sum_{m=-l}^{+l} F_l(r_{i\lambda}, \rho_\lambda) [l m \lambda] \langle l m \lambda | \quad (4)$$

where $[l m \lambda] \langle l m \lambda |$ is the spherical harmonic centered on λ . In the formalism of Muller et al.,^[35] this cutoff function is unique for a given atom, generally adjusted to reproduce the first ionization potential. The cutoff radii given in Table 1 were optimized to reproduce the ionization potentials and the lowest valence s, p, and d one-electron states as deduced from the tables of atomic data.

Table 2. Atomic transition energies of the Li, Na, Rb, and Cs atoms (in cm^{-1}).

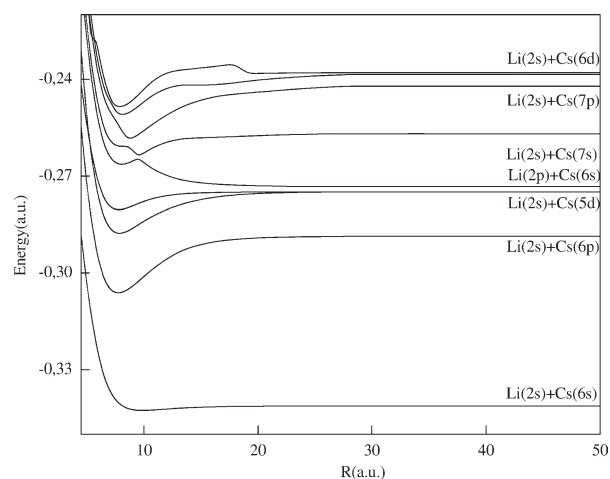
Atom	Atomic levels	This work	Experimental ^[36]	ΔE (cm^{-1})
Lithium	Li (2s)	0.00	0.00	0.00
	Li (2p)	14903.66	14903.66	0.00
	Li (3s)	27212.36	27206.12	6.24
	Li (3p)	30926.95	30925.38	1.53
	Li (3d)	31283.08	31283.08	0.00
Sodium	Na (3s)	0.00	0.00	0.00
	Na (3p)	169667.61	169667.61	0.00
	Na (4s)	25741.44	25739.80	1.64
	Na (3d)	29172.83	29172.83	0.00
	Na (4p)	30272.26	30270.65	1.61
Rubidium	Rb (5s)	0.00	0.00	0.00
	Rb (5p)	12737.87	12737.87	0.00
	Rb (4d)	19355.65	19355.65	0.00
	Rb (6s)	20,097	20102.92	5.92
	Rb (6p)	23,776	23781.92	5.92
Cesium	Cs (6s)	0.00	0.00	0.00
	Cs (6p)	11548.11	11548.11	0.00
	Cs (5d)	14557.92	14558.00	0.08
	Cs (7s)	18538.31	18535.98	2.33
	Cs (7p)	21880.02	21886.04	6.02

**Figure 1.** Potential energy curves for the $1\Sigma^+$ states of the LiCs molecule.

The Gaussian type orbital basis sets on Li, Na, and X atoms are 6s/5p/4d/2f, 7s/5p/3d/1f, 8s/6p/5d/2f, and 8s/5p/5d/2f, respectively, and the core-dipole polarizability of Li^+ , Na^+ , and X^+ are 0.1915, 0.993, and $9.075 a_0^3$, respectively.

In Table 2, a comparison between our *ab initio* and the experimental^[36] energy levels for Na (3s, 3p, 4s, 3d, and 4p), Li (2s, 2p, 3s, and 3p), Rb (5s, 5p, 6s, 4d, and 6p), and Cs (6s, 6p, 5d, 7s, 7p, and 6d) atomic states are presented. Our atomic energies are in good agreement with the experimental ones. The difference between our work and the experimental values does not exceed 6.24 cm^{-1} . Such atomic accuracy will be transmitted to the molecular calculations.

These agreements show the validity and the high accuracy of the use of these bases. The core-core interaction is evaluated as the ground state energy for the molecular ion instead of the approximation $1/R$, which is not accurate enough for this species, at least for small values of the internuclear distance. Semiempirical spin orbit pseudopotentials have been designed for Li, Na, and X atoms to reproduce the experimental splitting. The present investigation of the electronic structure for the molecular LiX and NaX has been performed

**Figure 2.** Potential energy curves for the $3\Sigma^+$ states of the LiCs molecule.

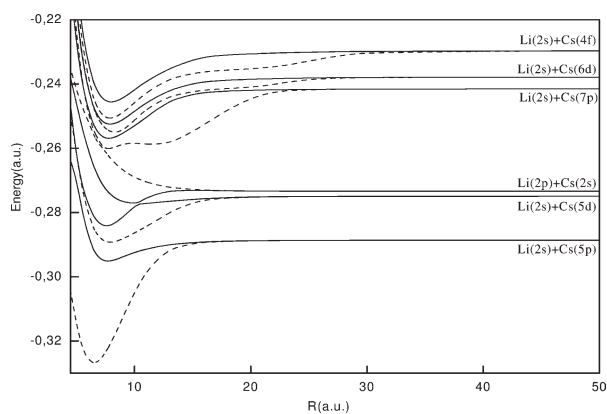


Figure 3. Potential energy curves for the $^1\Pi$ (solid lines) and $^3\Pi$ (dashed lines) states of the LiCs molecule.

by using the package configuration interaction (CI) by perturbation of a multiconfiguration wave function with spin orbit interaction of the Laboratoire de Physique Quantique Toulouse, France, which allows a full CI calculation.

Results

Potential energy curves and spectroscopic constants for the LiRb and LiCs molecules

Many articles^[17–22] have been devoted to the theoretical evaluation of the spectroscopic constants of alkali dimer, using the single and double configuration interaction methods.

Recently, *ab initio* calculations have greatly helped in the search and identification of new molecules because the experimental observation of new molecular species, either in laboratory or in space, are usually guided by knowledge of spectroscopic constants. Many articles^[17–22] have been devoted to the theoretical evaluation of the spectroscopic constants of alkali dimer, using the single and double configuration interaction methods. However, these authors use in their studies many other methods to determine the adiabatic potential curves and moments for the ground state and excited states. They have reduced the system to a two-electron problem using pseudopotentials supplemented by core-polarization potential for an atom.

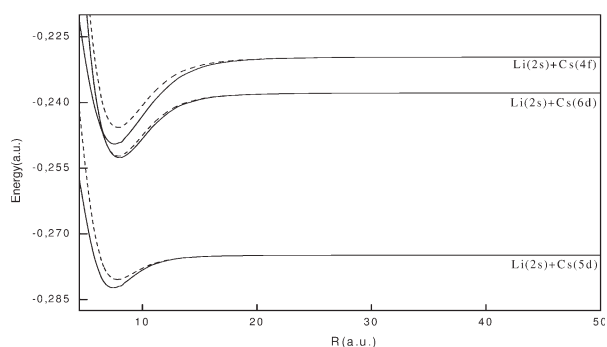


Figure 4. Potential energy curves for the $^1\Delta$ (solid lines) and $^3\Delta$ (dashed lines) states of the LiCs molecule.

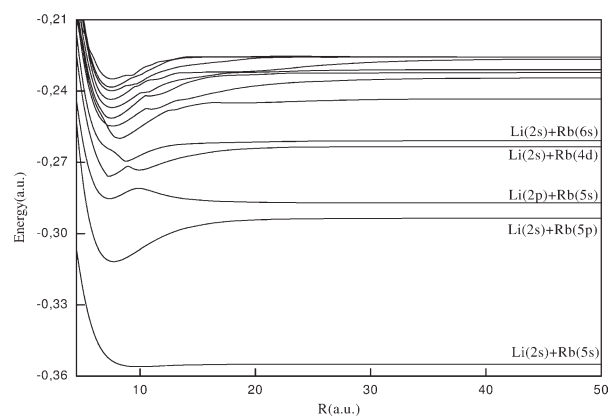


Figure 5. Potential energy curves for the $^3\Sigma^+$ states of the LiRb molecule.

The potential energy curves are shown for the $^1,3\Sigma^+$, $^1,3\Pi$, and $^1,3\Delta$ molecular states in Figures 1–4 of the LiRb and in Figures 5–8 of the LiCs molecules, respectively, dissociating into Li (2s, 2p) + Rb (5s, 5p, 6s, 4d, and 6p) and Li (2s, 2p) + Cs (6s, 6p, 5d, 7s, 7p, and 6d). They have been calculated for a large and dense grid of interatomic distances from 4.5 to 200 au to display the long-range avoided crossings. The spectroscopic constants for the $^1,3\Sigma^+$, $^1,3\Pi$, and $^1,3\Delta$ states for LiCs and LiRb are presented in Tables 3–8, respectively. The energies calculated at a large value of R using the present method are reported in Table 2 in comparison with the experimental dissociation limit energies. The only possible comparison with the experimental results relates to the fundamental state $X^1\Sigma^+$ and the highly excited states of $^1\Sigma^+$. The largest differences are smaller than 6.24 cm^{-1} for both LiRb and LiCs. This, in fact, represents the accuracy of the present calculations at the atomic level and can be regarded as a limit for the present molecular calculations.

To verify the accuracy of our calculated potential energy curves for states already studied, we calculated the spectroscopic constants of the ground states and the higher excited and we have compared with the available theoretical work.^[17–22] The main spectroscopic constants have been determined here as the equilibrium distance R_e , the potential well depth D_e and the vertical transition at the equilibrium distance of

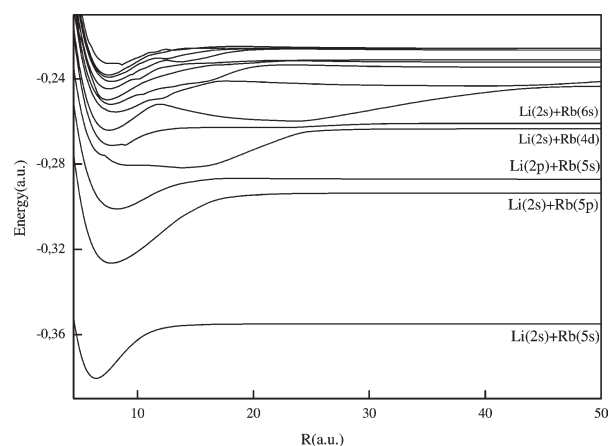


Figure 6. Potential energy curves for the $^1\Sigma^+$ states of the LiRb molecule.

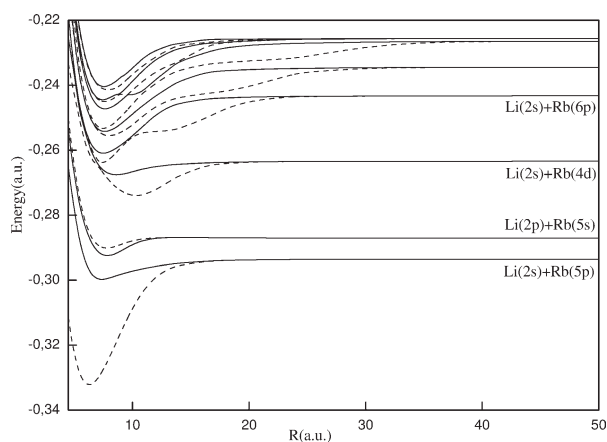


Figure 7. Potential energy curves for the 1Π (solid lines) and 3Π (dashed lines) states of the LiRb molecule.

the ground state for T_e . These spectroscopic constants (R_e , D_e , and T_e) for the $1\Sigma^+$ states are presented in Tables 3 and 6 and compared with the ones available in the literature. The ground state has been the most studied one, and a comparison can be done to experimental^[24,25] as well as previous theoretical results.^[18,23] There is a good agreement with the experimental data, with relative differences of about 0.2%, as well as with the previous theoretical estimations. This agreement gives confidence in the present calculation. As can be seen in Tables 3 and 6 for the other states also, our results are in good agreement with the experimental data, being generally better than the previous theoretical results. This is particularly true for the second excited state, where noticeable improvement can be observed for R_e and D_e . We find for example the ground state an equilibrium distance $R_e = 6.82$ au, whereas Mabrouk et al.^[17] and Korek et al.^[18] found 6.78 and 6.79 au, respectively. The same good agreement is observed between our other spectroscopic constants $D_e = 6014$ cm^{-1} and those found by Mabrouk et al.^[17] and Korek et al.^[18] for $D_e = 6032$ cm^{-1} and $D_e = 5996$ cm^{-1} , respectively. The six $1\Sigma^+$ adiabatic states for LiCs present double minima, the same result is found by Mabrouk et al.^[17] As said in their paper, the cutoff parameters were adjusted to reproduce the experimental dissociation

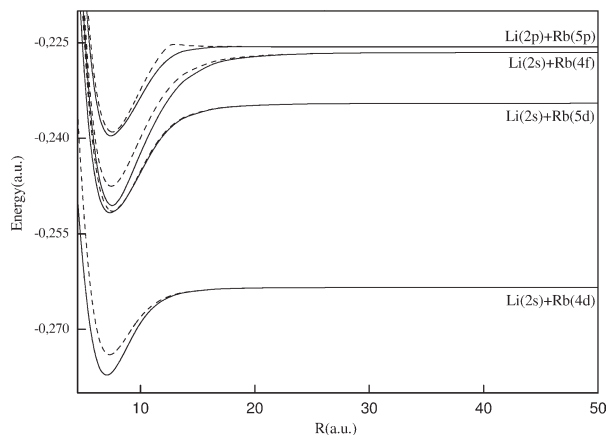


Figure 8. Potential energy curves for the 1Δ (solid lines) and 3Δ (dashed lines) states of the LiRb molecule.

Table 3. Spectroscopic constants of the $1\Sigma^+$ states of the LiRb molecule.

States	R_e (au)	D_e (cm^{-1})	T_e (cm^{-1})	Reference
1 1Σ	6.42	5606	0.00	This work
	6.34		0.00	Ref. [19]
	6.38		0.00	Ref. [20]
	6.46		0.00	Ref. [21]
2 1Σ	7.74	7226	11,865	This work
	7.77		11,639	Ref. [19]
3 1Σ	8.23	3120	17,450	This work
	8.00		17,348	Ref. [19]
4 1Σ	9.60	3776	21,924	This work
5 1Σ	7.83	2270	23,979	This work
6 1Σ				
1st min	7.56	4559	25,556	This work
2nd min	23.65	3624		This work
7 1Σ	8.07	4619	27,424	This work
8 1Σ	7.73	4345	28,209	This work
9 1Σ	7.43	4135	28,686	This work
10 1Σ	7.53	3994	32,976	This work
11 1Σ	7.78	3333	30,565	This work
12 1Σ	7.55	2978	31,007	This work

energy and the *ab initio* theoretical equilibrium distances. The spectroscopic constants for the excited states are presented here and compared with the available calculations, to the best of our knowledge; there are no experimental results for the excited states. For LiRb, the lowest energy states (1, 2, 3) $1\Sigma^+$ and $2^3\Sigma^+$, $1^1\Pi$, and (1, 2, 3, and 4) $1^3\Delta$ are bound with regular energy curves, whereas for LiCs the energy curve for the bound (1, 2) $1\Sigma^+$, $1^3\Pi$, and (1, 2, 3) $1^3\Delta$ state is also regular. The lowest energy states (6 and 4) $1^3\Sigma^+$ presents double minima, with a well at very large distances and another one at short distance. Both minima can trap vibrational states. The spectroscopic constants of the $3^1\Pi$ and $1^3\Delta$ states are presented in Tables 7 and 8. For all these states of different symmetries, many avoided crossings have been located at large internuclear distance as well as at short distance. Their existences will generate large nonadiabatic coupling and lead to an undulating behavior of the higher excited states at large internuclear distances. For the ground state of LiRb, a good

Table 4. Spectroscopic constants of the $3\Sigma^+$ states of the LiRb molecule.

States	R_e (au)	D_e (cm^{-1})	T_e (cm^{-1})	Reference
1 3Σ	9.88	238	5568	This work
	9.68		5678	Ref. [19]
2 3Σ	7.72	3999	14,983	This work
	7.68		14,719	Ref. [19]
3 3Σ	7.34		20,900	This work
4 3Σ				
1st min	7.23	2745	22,954	This work
2nd min	9.96	2165		
5 3Σ	8.80	1914	24,335	This work
6 3Σ	8.23	3645	26,469	This work
7 3Σ	7.66	4429	27,613	This work
8 3Σ	7.53	4209	28,345	This work
9 3Σ	7.54	3511	29,309	This work
10 3Σ	7.47	3733	30,067	This work
11 3Σ	7.55	3122	30,863	This work
12 3Σ	7.52	2782	31,202	This work

Table 5. Spectroscopic constants of the Π and Δ states of the LiRb molecule.

States	R_e (au)	D_e (cm $^{-1}$)	T_e (cm $^{-1}$)	Reference
1 $^1\Pi$	7.35	1363	17,717	This work
	7.20		17,205	Ref. [19]
2 $^1\Pi$	7.774	671	19,321	This work
	7.75		19,201	Ref. [19]
3 $^1\Pi$	8.59	918	24,780	This work
	8.65		24,295	Ref. [19]
1 $^3\Pi$	6.28	8482	10,604	This work
	6.327		10,233	Ref. [19]
2 $^3\Pi$	7.84	1188	19,838	This work
	7.777		19,484	Ref. [19]
3 $^3\Pi$	10.33	2303	23,395	This work
1 $^1\Delta$	7.03	3028	22,671	This work
	13.288	22,275	Ref. [19]	
2 $^1\Delta$	7.30	3769	28,273	This work
	13.779		27,936	Ref. [19]
3 $^1\Delta$	7.52	4617	28,524	This work
1 $^3\Delta$	7.29	2319	23,379	This work
	13.851		23,029	Ref. [19]
2 $^3\Delta$	7.57	3719	28,322	This work
	14.305		28,142	Ref. [19]
3 $^3\Delta$	7.44	5276	29,183	This work

agreement is obtained with previous pseudopotential CI calculations^[19–21] for R_e with relative differences being smaller than 0.6%. The comparison of our results for spectroscopic con-

Table 6. Spectroscopic constants of the $^1\Sigma^+$ states of CsLi molecule.

States	R_e (au)	D_e (cm $^{-1}$)	T_e (cm $^{-1}$)	Reference
1 $^1\Sigma$	6.82	6014.26	0.00	This work
	6.78	6032.0	0.00	Ref. [17]
	6.79	5996.0	0.00	Ref. [18]
	6.89	5875.455	0.00	Exp. [23]
		5990 \pm 170	0.00	Exp. [24]
2 $^1\Sigma$	8.27	6861.0	10,718	This work
	8.28	6865.0	10,715	Ref. [17]
	8.27	6879.0	10,664	Ref. [18]
3 $^1\Sigma$	8.15	3628	16,932	This work
	8.16	3659	16,932	Ref. [17]
	8.14	3670	16,865	Ref. [18]
4 $^1\Sigma$	9.45	1609.87	19,081	This work
	9.41	1856	19,081	Ref. [17]
	9.42	1908	18,998	Ref. [18]
5 $^1\Sigma$	8.31	1753.34	21293.04	This work
	7.9	2924	21,647	Ref. [17]
Second min	18.49	3168	21,403	
	7.9	3156	21,618	Ref. [18]
6 $^1\Sigma$	7.87	3071.55	25083.84	This work
Second min	18.52	3317		
	7.87	3773	24,140	Ref. [17]
Second min	25.78	3241		
	7.87	3830	24,119	Ref. [18]
7 $^1\Sigma$	7.91	3676	24841.88	This work
	8.63	3387	25,331	Ref. [17]
Second min	42.78	807	27,911	
Third min	48.56	848	27,870	
	8.57	3370	25,316	Ref. [18]
8 $^1\Sigma$	8.66	3401	27261.54	This work
	8.13	4072	26,283	Ref. [17]
Second min	58.75	1700	28,655	
9 $^1\Sigma$	8.12	4055	26,285	This work
	7.88	3604	26,913	Ref. [17]

Table 7. Spectroscopic constants of the $^3\Sigma^+$ states of CsLi molecule.

States	R_e (au)	D_e (cm $^{-1}$)	T_e (cm $^{-1}$)	Reference
1 $^3\Sigma$	9.84	308	5727	This work
	9.83	308	5725	Ref. [17]
	9.83	307		Ref. [18]
	9.864	309		Exp. [23]
2 $^3\Sigma$	7.70	13,730	13,730	This work
	7.71	3851	13,730	Ref. [17]
	7.71		13,682	Ref. [18]
3 $^3\Sigma$	7.84	2785	17,779	This work
	7.81	2812	17,779	Ref. [17]
	7.84		17,712	Ref. [18]
4 $^3\Sigma$	8.06	1206	22,468	This work
	8.02		22,467	Ref. [17]
	8.03		22,451	Ref. [18]
5 $^3\Sigma$	9.56	1452	23,100	This work
	9.51	1472	23,099	Ref. [17]
6 $^3\Sigma$	8.72	3579	24,235	This work
	8.73	3676	24,237	Ref. [17]
7 $^3\Sigma$	8.10	3145.64	25,865	This work
	8.08	2849	25,869	Ref. [17]
	8.03		25,809	Ref. [18]
8 $^3\Sigma$	7.87	3943	26,397	This work
	7.84	3945	26,410	Ref. [17]
9 $^3\Sigma$	7.89	2256.03	27,405	This work
1st min	7.88	2894	27,623	Ref. [17]
2nd min	24.17	187		

stants (R_e and D_e) of two molecules LiRb and LiCs shows that the well depth and equilibrium distance for LiCs are more bound than obtained for LiRb. Values for the internuclear equilibrium distance R_e , the minimum-to-minimum electronic excitation energy T_e , and the well depth D_e were determined from vibrational energies $G(v)$.

As can be seen in Tables 3–5, our improved results for the main spectroscopic constants are in good agreement with the experimental data. A comparable accuracy was obtained by the calculations of Korek et al.,^[18] which used similar methods [pseudopotential and core potential potentials (CPP)]. All electrons calculations did not get significative improvement, leading globally to too long R_e , too small D_e . In all electrons approaches, there is a lack of attractive effects related to difficulties in the estimation of electronic correlation, whereas using pseudopotential and CPP parameterized semiempirically on the atomic spectrum, some compensation occurs. The accurate calculation of these main spectroscopic constants for the heavier alkali dimers is still an open challenge. The use of pseudopotential is not the best way here to reach spectroscopic accuracy; however, the diabatization method actually requires a full CI calculation, which becomes prohibitive for all electron approaches.

In these calculations, for LiRb, we used 6.941 for Li and 85.4676 for Rb as atomic masses, respectively, whereas for the isotopomer ^{23}Na ^{38}Rb , we used 22.9897677 for Na and 84.911794 for Rb as atomic masses, respectively.

Potential energy curves and spectroscopic constants for the NaRb and NaCs molecules

In our previous study on NaRb and NaCs, potential energy curves and relevant permanent dipole moments have been

Table 8. Spectroscopic constants of the Π and Δ states of the CsLi molecule.

States	R_e (au)	D_e (cm $^{-1}$)	T_e (cm $^{-1}$)	Reference
$1^1\Pi$	7.72	1420	16,160	This work
	7.711	1415	16,165	Ref. [17]
	7.756		15,133	Ref. [18]
$2^1\Pi$	7.79	1595.495	16012.217	Exp. [25]
	7.601	2025	18,577	This work
	7.59	2021	18,570	Ref. [17]
	7.575		18,542	Ref. [18]
	7.663	2178.93	18293.37	Exp. [25]
$3^1\Pi$	9.913	804	20,129	This work
	9.903	813	20,123	Ref. [17]
	7.728		20,095	Ref. [18]
$1^3\Pi$	6.510	8359	9222	This work
	7.711	1415	16,165	Ref. [17]
	7.756		16,133	Ref. [18]
$2^3\Pi$	7.915	3144	17,447	This work
	7.590	2021	18,570	Ref. [17]
	7.575		18,542	Ref. [18]
$3^3\Pi$	28.295	Repulsive	20,932	This work
	9.911	813	20,123	Ref. [17]
	7.728		20,095	Ref. [18]
	7.450	1626	18,965	This work
	7.450	1628	18,963	Ref. [17]
$2^1\Delta$	7.491		19,036	Ref. [18]
	8.12	3238	25,485	This work
	8.000	3232	25,486	Ref. [17]
$3^1\Delta$	7.987		25,698	Ref. [18]
	7.560	4349	26,168	This work
	7.560	4352	26,164	Ref. [17]
$1^3\Delta$	7.493		26,584	Ref. [18]
	7.809	1209	19,383	This work
	7.809	1209	19,381	Ref. [17]
$2^3\Delta$	7.871		19,430	Ref. [18]
	7.881	3154	25,565	This work
	7.900	3153	25,565	Ref. [17]
$3^3\Delta$	6.739		26,950	Ref. [18]
	7.862	3514	27,005	This work
	7.860	3513	27,003	Ref. [17]
	7.724		28,216	Ref. [18]

computed from 5 to 200 au for all electronic states correlated up to Na(4p) + Rb(6p) and Na(4p) + Cs(6d). Here, we have considered a somewhat larger range of internuclear distances by adding some points at short R . Moreover, the R step presently used is equal to 0.25 au between 4.50 and 12 au, 0.5 au between 12 and 20 au, 1 au between 20 and 30 au, and 10 au between 30 and 200 au. Calculations now cover the range from 4.5 to 200 au, and they have been extended to electronic states correlated to Na (4p) + Rb (6p) and Na (4p) + Cs (6d). As potential energy curves for electronic states are judged sufficiently accurate, we also report corresponding spectroscopic constants.

In Tables 9–13, we present new values for spectroscopic constants deduced from rovibrational energies, permanent dipole moment determined at the equilibrium position are also given. Good agreement is obtained with recent experimental data of Kasahara et al.^[26] and those of the Wang et al.^[28] obtained for various highly excited states for which the potential energy curves can have curious patterns due to avoided crossings at short R or to ionic covalent interactions at large internuclear distance.

Table 9. Spectroscopic constants of the $^1\Sigma^+$ states of the NaRb molecule.

States	R_e (au)	D_e (cm $^{-1}$)	T_e (cm $^{-1}$)	Reference
$1^1\Sigma$	6.80	4848	0.00	This work
	7.01		0.00	Ref. [19]
	6.86		0.00	Ref. [20]
	6.96	5263	0.00	Ref. [21]
	6.78		0.00	Ref. [22]
	6.84		0.00	Exp. [26]
$2^1\Sigma$	8.27	6025	11,454	This work
	8.27		11,396	Ref. [19]
	8.20	6578	1764	Ref. [22]
$3^1\Sigma$	8.40	4255	17,460	This work
	8.41		17,315	Ref. [19]
	8.34	4525	17,704	Ref. [22]
$4^1\Sigma$	9.68	3247	20,967	This work
$5^1\Sigma$	8.13	1928	23,012	This work
$6^1\Sigma$				
1st min	8.65	3599	24,893	This work
2nd min	22.51	3287		
	8.12	4067	24,941	Ref. [22]
			24857.81	Exp. [27]
$7^1\Sigma$	8.47	4324	26,228	This work
$8^1\Sigma$	8.24	3329	27,258	This work
	8.30	3112	27,498	Ref. [22]
$9^1\Sigma$	8.10	3521	27,613	This work
	8.13	3558	27,462	Ref. [22]
$10^1\Sigma$	8.19	2293	28,709	This work
$11^1\Sigma$	8.30	2798	29,507	This work
$12^1\Sigma$	8.15	2775	29,930	This work
$13^1\Sigma$	8.26	3415	30,131	This work

Table 10. Spectroscopic constants of the $^3\Sigma^+$ states of the NaRb molecule.

States	R_e (au)	D_e (cm $^{-1}$)	T_e (cm $^{-1}$)	Reference
$1^3\Sigma$	10.70	194	4653	This work
	11.21		4363	Ref. [19]
	10.21	284	4978	Ref. [22]
	8.246		4847.75	Exp. [28]
$2^3\Sigma$	8.67	2155	15,324	This work
	8.67		15,202	Ref. [19]
	8.41	2444	15,634	Ref. [22]
$3^3\Sigma$				
1st min	7.79	1848	19,967	This work
2nd min	12.67	1128		
	7.85		19,837	Ref. [19]
	7.59	2126	20,104	Ref. [22]
$4^3\Sigma$	8.12	2098	22,116	This work
	8.16	1390	23,226	Ref. [22]
$5^3\Sigma$				
1st min	8.27	208	24,732	This work
2nd min	10.53	1028		
$6^3\Sigma$	9.17	2928	25,689	This work
$7^3\Sigma$	8.68	3960	26,592	This work
$8^3\Sigma$	8.33	3348	27,239	This work
$9^3\Sigma$	7.94	2881	28,253	This work
$10^3\Sigma$				
1st min	7.90	3250	29,055	This work
2nd min	19.12	1081		
$11^3\Sigma$	7.87	3019	29,686	This work
$12^3\Sigma$	7.85	3494	30,053	This work
$13^3\Sigma$	8.17	3289	30,598	This work

The calculated potential energy curves of the singlet states of NaRb and NaCs, correlating with dissociation limits up to Na (4p) + Rb (6p) and Na (4p) + Cs (6d), have been plotted in

Table 11. Spectroscopic constants of the $1\Sigma^+$ states of NaCs molecule.

States	R_e (au)	D_e (cm $^{-1}$)	T_e (cm $^{-1}$)	Reference
1 1Σ	7.19	4905	0.00	This work
	7.20			Ref. [18]
2 1Σ	8.72	5979	10,473	This work
	8.47		10,511	Ref. [18]
3 1Σ	8.45	2798	16,656	This work
	8.34		16,665	Ref. [18]
4 1Σ	9.05	3141	18,996	This work
	8.57		19,068	Ref. [18]
5 1Σ	8.54	1768	20,685	This work
	8.27		20,887	Ref. [18]
6 1Σ				
1st min	8.45	3230	23,553	This work
2nd min	23.45	3132		
	8.45		23,582	Ref. [18]
7 1Σ	8.38	2578	24,930	This work
	8.80		24,659	Ref. [18]
8 1Σ	8.60	3610	25,617	This work
9 1Σ	8.40	3263	26,125	This work

Figures 11–16. These potentials energies have been calculated employing effective-core-polarization potentials and valence-CI calculations. For these systems, we produced exact potential energy in the basis set as we performed a full CI according to the number of electrons does not exceed two. The potentials of the ground states for NaRb and NaCs do not show any double minima; however, they do show differences from the potential energy curve of the ground state of the cation along with the lowest excited state of the cation, implying that they are not simple Rydberg states over the different values R but change in character at different R . The present results are in generally good agreement with the previous theoretical and experimental results. In the present calculations, the equilibrium bond lengths are slightly overestimated, whereas the well depths are in some cases are slightly underestimated.

For example, we found for the ground state an equilibrium distance $R_e = 6.80$ au, for NaRb, whereas Korek et al.^[19] and Igel-Mann et al.^[20] found 7.01 and 6.86 au, respectively. The same good agreement is observed between our results spectroscopic constants (6.80 au) and experimental results of Kasahara et al.^[26] (6.84 au). Recent theoretical Coupled Cluster (CC) calculations have been performed in Refs.^[19,20].

Table 12. Spectroscopic constants of the $3\Sigma^+$ states of NaCs molecule.

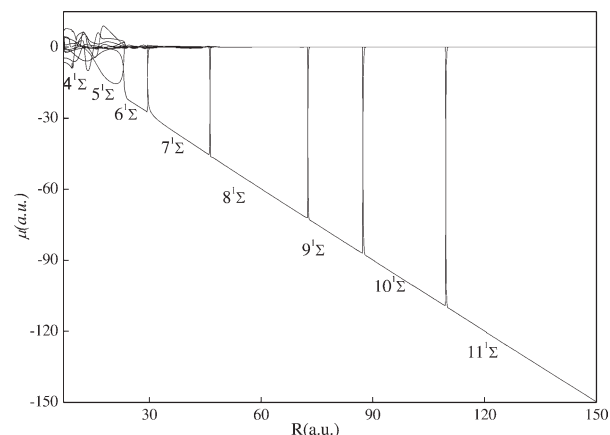
States	R_e (au)	D_e (cm $^{-1}$)	T_e (cm $^{-1}$)	Reference
1 3Σ	10.896	210	4695	This work
2 3Σ	8.810	1903	14,548	This work
	8.712		14,538	Ref. [18]
3 3Σ	8.083	2531	16,933	This work
	8.078		16,919	Ref. [18]
4 3Σ				This work
1st min	8.304	952	20,884	
2nd min	14.82	434		Ref. [18]
	8.490	21,698		
5 3Σ	8.428	275	23,168	This work
6 3Σ	8.801	2153	24,629	This work
7 3Σ	8.908	2556	25,047	This work
8 3Σ	8.713	3523	25,702	This work

Table 13. Spectroscopic constants of the Π and Δ states of the NaCs molecule.

States	R_e (au)	D_e (cm $^{-1}$)	T_e (cm $^{-1}$)	Reference
1 1Π	8.295	1117	15,336	This work
	8.280		15,341	Ref. [18]
2 1Π	7.962	1010	18,453	This work
	7.947		18,470	Ref. [18]
3 1Π	12.05	321	21,516	This work
	11.141		20,047	Ref. [18]
1 3Π	7.100	6208	10,244	This work
	7.062		10,277	Ref. [18]
2 3Π	8.303	2725	16,738	This work
	8.312		16,737	Ref. [18]
3 3Π	9.231	1861	19,975	This work
1 1Δ	7.988	1316	18,147	This work
	7.966		18,252	Ref. [18]
2 1Δ	8.350	3033	24,757	This work
	8.344		24,730	Ref. [18]
3 1Δ	8.155	3756	25,632	This work
	8.115		26,084	Ref. [18]
1 3Δ	8.200	1062	18,405	This work
	8.206		18,490	Ref. [18]
2 3Δ	8.250	2947	24,643	This work
	8.283		24,802	Ref. [18]
3 3Δ	8.310	3298	26,192	This work
	8.350		26,526	Ref. [18]

Figures 15 and 16 illustrate the singlet and triplet adiabatic Π and Δ states. Because these symmetries involve orbital's perpendicular to the molecular axis and overlapping only loosely, the adiabatic curves are rather flat. The singlet and triplet adiabatic Δ curves are almost degenerate. The spectroscopic constants (R_e , D_e , and T_e) of the bound states are given in Table 13.

As can be seen in Tables 9 and 11, our improved results for the binding energy and the equilibrium distance are in good agreement and being better than older theoretical results and comparable with the most recent ones. When compared with the recent ones results, our equilibrium distances are slightly too low because we use pseudopotentials and operator core-valence correlation estimates; some repulsive effects are clearly underestimated in our calculations. For better accuracy, pseudopotentials with smaller cores should be used.

**Figure 9.** Permanent dipole moments μ for the 14 low-lying $1\Sigma^+$ states of the LiRb molecule as a function of the internuclear distance.

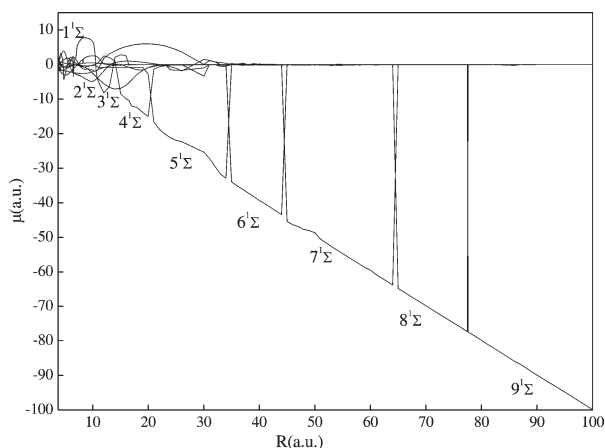


Figure 10. Permanent dipole moments μ for the eight low-lying $1\Sigma^+$ states of the LiCs molecule as a function of the internuclear distance.

Many avoided crossings for the higher excited states of NaRb and NaCs molecules have been located at large distance as well as at short distance. Their existences will generate large nonadiabatic coupling and lead to an undulating behavior of the higher excited states at large internuclear distances. To the best of our knowledge, there is no experimental information for the Π and Δ electronic states. As can be seen in Table 13, our R_e and T_e values are 8.295 au and 15,336 cm^{-1} for the $1^1\Pi$ state and 7.962 and 18,453 cm^{-1} for the $2^1\Pi$ state, respectively, to be compared with the calculation of Ref. [18] found 8.280 and 15,341 cm^{-1} as well as 7.947 and 18,470 cm^{-1} . Our values are in good agreement compared with those of [19,22]. A good agreement between our calculation and the other work [18] for the $2^1\Pi$ and $3^1\Pi$ states is observed.

Permanent dipole moments

The dipole moment can be considered as a sensitive test for the accuracy of the calculated electronic wave functions and energies. For this, we have determined the adiabatic permanent dipole moments for the large and dense grid of internuclear distances, from 4.5 to 200 au.

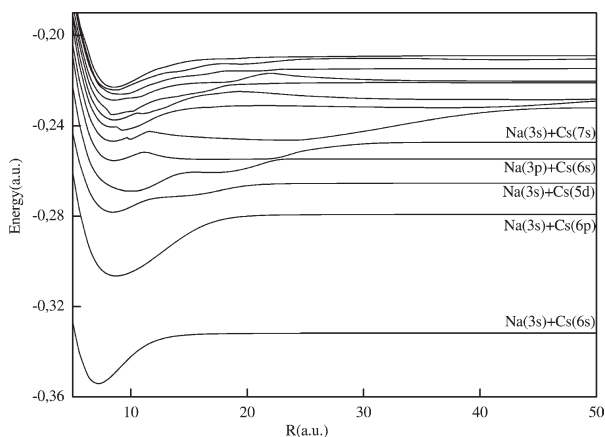


Figure 11. Potential energy curves for the $1\Sigma^+$ states of the NaCs molecule.

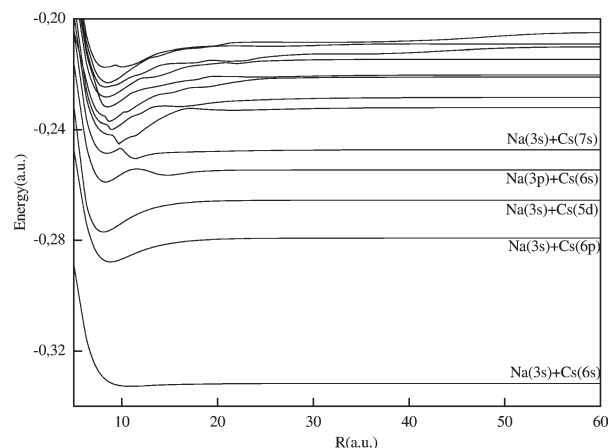


Figure 12. Potential energy curves for the $3\Sigma^+$ states of the NaCs molecule.

Figures 9 and 10 presents the adiabatic permanent dipole moment of the all states of $1\Sigma^+$ symmetry for both LiRb and LiCs molecules. The permanent dipole moment of these 1–4 $1\Sigma^+$ states does not behave as a pure linear function of R . But the dipole moment of these states, one after another, behaves as a linear function of R and then drops to zero at particular distances corresponding to the avoided crossings between the two neighbor electronic states. If these curves are combined, they produce piecewise the whole- R function due to the ionic character of these states. The discontinuities between the consecutive parts are due to the avoided crossings, in this behavior can be understood recalling that around 10.0 au the $1^1\Sigma^+$ and $2^1\Sigma^+$ states exchange their ionic character, whereas the X state keeps its neutral character.

This particular behavior can be easily understood from the diabatic potential and dipole curves. The permanent dipole gives actually a direct illustration of the ionic character of the adiabatic electronic wave function. We thus access directly a visualization of the R -dependence of the charge distribution of the wave function. The distance for which two consecutive adiabatic states have the same dipole locates the crossing of the

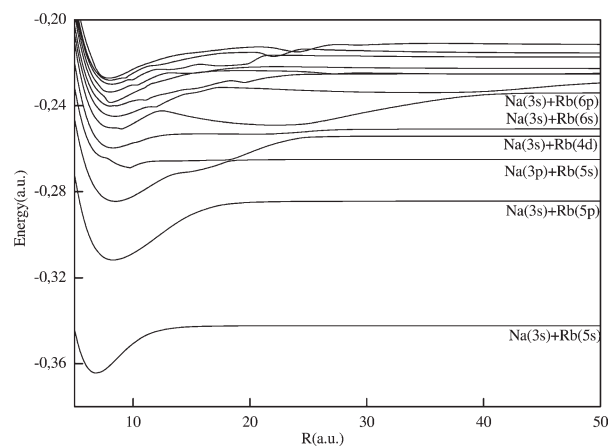


Figure 13. Potential energy curves for the $1\Sigma^+$ states of the NaRb molecule.

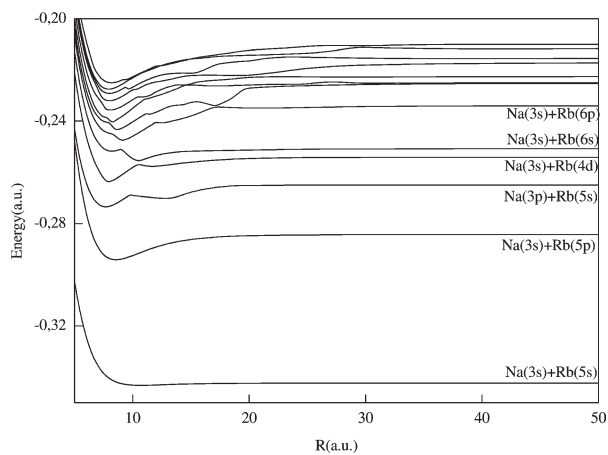


Figure 14. Potential energy curves for the $3\Sigma^+$ states of the NaRb molecule.

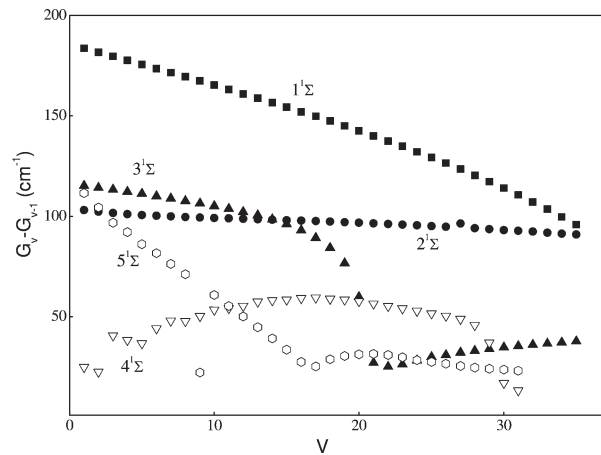


Figure 17. Vibrational level spacings for the $1\Sigma^+$ states of the CsLi system.

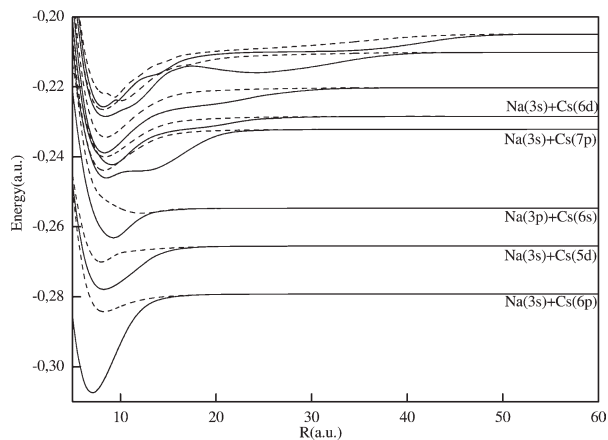


Figure 15. Potential energy curves for the 1Π (solid lines) and 3Π (dashed lines) states of the NaCs molecule.

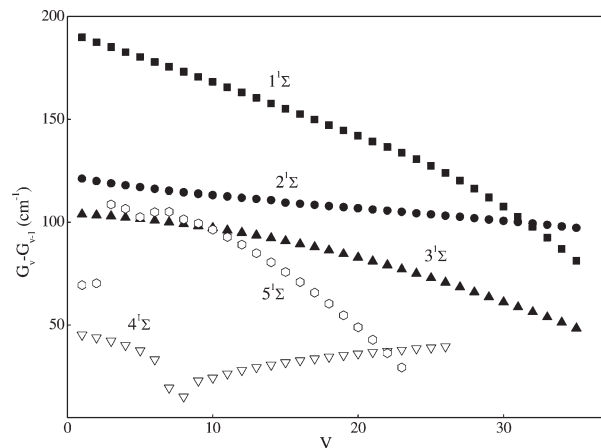


Figure 18. Vibrational level spacings for the $1\Sigma^+$ states of the RbLi system.

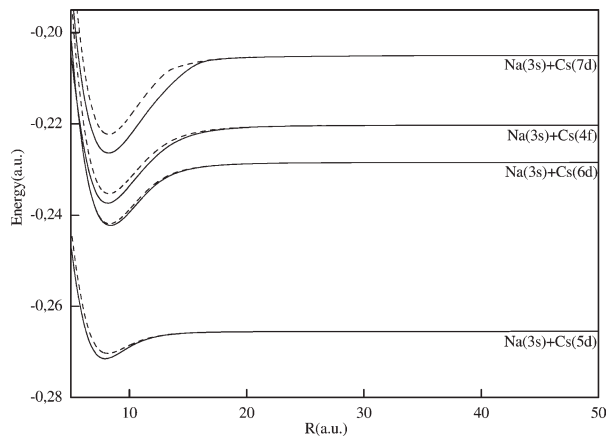


Figure 16. Potential energy curves for the 1Δ (solid lines) and 3Δ (dashed lines) states of the NaCs molecule.

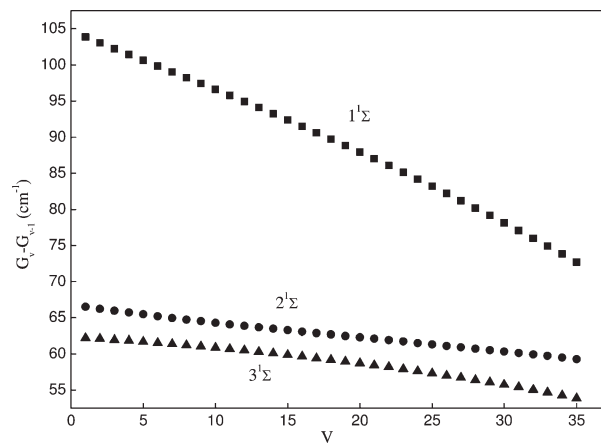


Figure 19. Vibrational level spacings for the $1\Sigma^+$ states of the NaRb system.

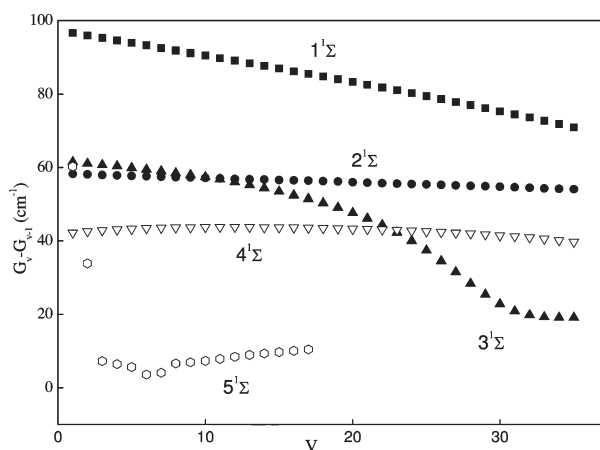


Figure 20. Vibrational level spacings for the $1\Sigma^+$ states of the NaCs system.

ionic diabatic state with the corresponding neutral one. The sharpness of the slopes around the node for the dipole is closely related to the weakness of the avoided crossing for energy.

The behavior of the matrix elements of the dipole moment determining the transitions illustrates the well-known relation between the radial coupling and dipole operators a relation, which allows one in a different context to introduce the electron translation factors.

We thus access directly a visualization of the R -dependence of the charge distribution of the wave function. The distance for which two consecutive adiabatic states have the same dipole locates the crossing of the ionic state with the corresponding neutral one. We have drawn for several $(1-5) 1,3\Sigma^+$, $1,3\Pi$, and $1,3\Delta$ states, in Figures 17–20, the vibrational-level spacing ($E_{v+1} - E_v$) according to the vibrational levels number V . We observe a roughly linear behavior, except for the highest levels approaching the dissociation limit.

Conclusions

In this article, we have presented an accurate calculation of the potential energy curves and their spectroscopic constants for the ground and numerous excited states for the neutral molecules LiX and NaX. The calculation method used in our study is based on a nonempirical pseudopotential approach for the Li, Na, and X cores. Furthermore, the energy obtained is corrected by including the core–core and core–valence correlations. The adiabatic potential energy curves of all electronic states and their spectroscopic constants of the LiX molecule dissociating into (Rb (5s, 5p, 6s, 4d, and 6p); Cs (6s, 6p, 5d, 7s, and 7p)) + Li (2s, 2p, 3s, and 3p) and those of the NaX molecule dissociating into Na (3s, 3p, 4s, 3d, and 4p) + (Rb (5s, 5p, 6s, 4d, and 6p); Cs (6s, 6p, 5d, 7s, and 7p)) have been calculated.

The unusual behavior of the adiabatic excited states could lead to interesting experimental effects accessible to spectroscopic techniques. As in LiH, all present a well nearly as deep as the interval between the asymptotic levels. Because of their

wide extension, these wells trap a large number of vibration levels. In addition to this principle, which exists for all states whose asymptote is less than the ionic Li^-X^+ and Na^-X^+ , there are other wells, shallow at short interatomic distances nuclear which could therefore be accessible by photoexcitation. The shape of these double wells suggests interesting spectroscopy and dynamics. Because these highly excited states are integrated into a variety of continuum and bound states, strong vibronic effects can also be provided, as is observed for LiH. This set of data can be further used to perform detailed spectroscopic studies including vibronic effects, radiative and nonradiative lifetimes. These studies allow us to view the important point on the R -dependence of the dipole moments can be obtained experimentally if the average value of the dipole is measured for a large number of vibration levels. So the information obtained for different adiabatic states can lead us to an experimental determination of the neutral–ionic diabatic crossing and crossing related to prevent potential curves. Another interesting aspect of these results is related to the external branch repulsion wells excited states corresponding to the ionic species. It has a considerable dipole (a few tenths of atomic energy unit) due to the large charge separation in the ionic state. These abnormally high values for the dipole moments should lead to interesting physical effects, such as the infrared spectrum.

Acknowledgments

The authors wish to thank the anonymous referees for their careful reading of the manuscript and their fruitful comments and suggestions.

- [1] W. C. Stwalley, H. Wang, *J Mol Spectrosc* 1999, 195, 194.
- [2] (a) O. Dulieu, F. Masnou-Seeuws, *J Opt Soc Am B* 2003, 20, 1083; (b) J. T. Bahns, P. L. Gould, W. C. Stwalley, *Adv At Mol Phys* 2000, 42, 71.
- [3] N. Balakrishnan, A. Dalgarno, *Chem Phys Lett* 2001, 341, 652.
- [4] E. Bodo, F. A. Gianturco, A. Dalgarno, *J Chem Phys* 2002, 116, 9222.
- [5] T. Rom, T. Best, O. Mandel, A. Widera, M. Greiner, T. W. Hansch, I. Bloch, *Phys Rev Lett* 2004, 93, 073002.
- [6] M. Kajita, *Eur Phys D* 2003, 23, 337.
- [7] R. V. Krems, *Int Rev Phys Chem* 2005, 24, 99.
- [8] A. V. Avdeenkov, M. Kajita, J. L. Bohn, *Phys Rev A* 2006, 73, 022707.
- [9] R. V. Krems, *Phys Rev Lett* 2006, 96, 123202.
- [10] D. Demille, *Phys Rev Lett* 2002, 88, 067901.
- [11] S. F. Yelin, K. Kirby, R. Cote, *Phys Rev A* 74, 050301 (R) (2006).
- [12] T. Kraemer, M. Mark, P. Walburger, J. G. Danzl, C. Chin, B. Engesser, A. D. Lange, K. Pilch, A. Jaakkola, H. C. Nagerl, R. Grimm, *Nature* 2006, 440, 315.
- [13] J. Doyle, B. Friedrich, R. Krems, F. Masnou-Seeuws, *Eur Phys J D* 2004, 31, 149.
- [14] O. Dulieu, M. Raoult, E. Tiemann, *J Phys B: At Mol Opt Phys* 2006, 39.
- [15] O. Dulieu, P. Pillet, *Isr J Chem* 2004, 44, 253.
- [16] M. Focault, Ph. Millié, J. P. Daudéy, *J Chem Phys* 1992, 96, 1257.
- [17] N. Mabrouk, H. Berriche, H. Ben Ouada, F. X. Gadea, *J Phys Chem A* 2010, 114, 6657.
- [18] M. Korek, A. R. Allouche, K. Fakhreddine, A. Chaalan, *Can J Phys* 2000, 78, 977.
- [19] M. Korek, A. R. Allouche, M. Kobeissi, A. Chaalan, M. Dagher, K. Fakherddin, M. Aubert-Frecon, *Chem Phys* 2000, 256, 1.
- [20] G. Igel-Mann, U. Wedig, P. Fuentealba, H. Stoll, *J Chem Phys* 1986, 84, 5007.
- [21] M. Urban, A. J. Sadlej, *J Chem Phys* 1995, 103, 9692.
- [22] M. Korek, O. Fawwaz, *Int J Quantum Chem* 2009, 109, 938.

- [23] P. Staunum, A. Pashov, H. Knockel, E. Tieman, *Phys Rev A* 2007, 75, 042513.
- [24] Thermodynamic Properties of Individual Substances, Vol. 4, Book 2 [in Russian]; Nauka: Moscow; p. 982.
- [25] A. Stein, A. Passhov, P. F. Staunum, H. Hnocker, E. Tiemann, *Eur Phys J D* 2008, 48, 177.
- [26] S. Kasahara, T. Elbi, M. Tanimura, H. Koma, K. Matsubara, M. Baba, H. Kato, *J Chem Phys* 1996, 105, 1241.
- [27] P. Korytko, W. Jastrzebski, P. Kowalczyk, *Chem Phys Lett* 2005, 404, 323.
- [28] Y. C. Wang, M. Kajitani, S. Kasahara, M. Baba, K. Ishikawa, H. Kato, *J Chem Phys* 1991, 95, 6229.
- [29] J. C. Barthelat, Ph. Durand, A. Serafini, *Mol Phys* 1975, 33, 179.
- [30] J. C. Barthelat, Ph. Durand, *Gazz Chim Ital* 1978, 108, 255.
- [31] N. Khelifi, B. Oujia, F. X. Gadea, *J Chem Phys* 2002, 116, 2879.
- [32] N. Khelifi, W. ZRafi, B. Oujia, F. X. Gadea, *Phys Rev A* 2002, 65, 042513.
- [33] W. ZRafi, N. Khelifi, B. Oujia, F. X. Gadea, *J Phys B: At Mol Opt Phys* 2006, 39, 3815.
- [34] N. Khelifi, *J Russ Laser Res* 2008, 29, 274.
- [35] W. Muller, J. Flesch, W. Meyer, *J Chem Phys* 1984, 80, 3297.
- [36] C. E. Moore, Atomic Energy Levels, National Bureau of Standards Circular, No. 467; U.S. GPO: Washington, DC, 1971.

Received: 3 May 2011
Revised: 26 September 2011
Accepted: 27 September 2011
Published online on